HHS Public Access

Author manuscript

Biochim Biophys Acta. Author manuscript; available in PMC 2018 January 01.

Published in final edited form as:

Biochim Biophys Acta. 2017 January ; 1861(1 Pt A): 3388–3398. doi:10.1016/j.bbagen.2016.08.021.

A highly prevalent equine glycogen storage disease is explained by constitutive activation of a mutant glycogen synthase

C.A. Maile[1], **J. R. Hingst**[2], **K. K. Mahalingan**[3], **A. O. O'Reilly**[4], **M. E. Cleasby**[5], **J. R. Mickelson**[6], **M. E. McCue**[7], **S. M. Anderson**[7], **T. D. Hurley**[3], **J. F. P. Wojtaszewski**[2], and **R. J. Piercy**[1]

[1]Comparative Neuromuscular Diseases Laboratory, Department of Clinical Sciences and Services, Royal Veterinary College, London, UK

[2]Department of Nutrition, Exercise and Sports, Faculty of Science, University of Copenhagen, Denmark

[3]Department of Biochemistry and Molecular Biology, Indiana University School of Medicine, Liverpool John Moores University, Liverpool, UK

[4]School of Natural Sciences and Psychology, Liverpool John Moores University, Liverpool, UK

[5]Department of Comparative Biomedical Sciences, Royal Veterinary College, London, UK

[6]Veterinary Biomedical Sciences Department, University of Minnesota, St. Paul, MN, USA

[7]Veterinary Population Medicine Department, University of Minnesota, St. Paul, MN, USA

Summary

BACKGROUND—Equine type 1 polysaccharide storage myopathy (PSSM1) is associated with a missense mutation (R309H) in the glycogen synthase (*GYS1*) gene, enhanced glycogen synthase (GS) activity and excessive glycogen and amylopectate inclusions in muscle.

METHODS—Equine muscle biochemical and recombinant enzyme kinetic assays *in vitro* and homology modelling *in silico*, were used to investigate the hypothesis that higher GS activity in affected horse muscle is caused by higher GS expression, dysregulation, or constitutive activation via a conformational change.

RESULTS—PSSM1-affected horse muscle had significantly higher glycogen content than control horse muscle despite no difference in GS expression. GS activity was significantly higher in muscle from homozygous mutants than from heterozygote and control horses, in the absence and presence of the allosteric regulator, glucose 6 phosphate (G6P). Muscle from homozygous mutant horses also had significantly increased GS phosphorylation at sites 2+2a and significantly higher AMPKα1 (an upstream kinase) expression than controls, likely reflecting a physiological attempt

Corresponding author: Professor Richard Piercy, Comparative Neuromuscular Diseases Laboratory, Department of Clinical Sciences and Services, The Royal Veterinary College, Royal College Street, London, NW1 0TU. UK. Tel: 0044 207 468 5000 rpiercy@rvc.ac.uk.

to reduce GS enzyme activity. Recombinant mutant GS was highly active with a considerably lower K_m for UDP-glucose, in the presence and absence of G6P, when compared to wild type GS, and despite its phosphorylation.

CONCLUSIONS—Elevated activity of the mutant enzyme is associated with ineffective regulation via phosphorylation rendering it constitutively active. Modelling suggested that the mutation disrupts a salt bridge that normally stabilises the basal state, shifting the equilibrium to the enzyme's active state.

GENERAL SIGNIFICANCE—This study explains the gain of function pathogenesis in this highly prevalent polyglucosan myopathy.

Graphical abstract

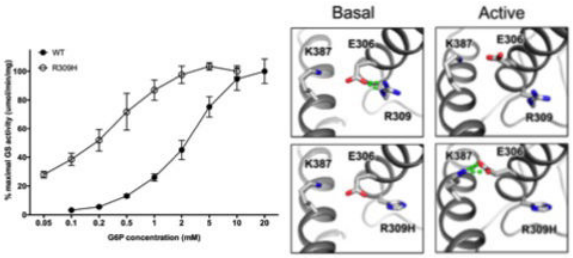

Keywords

PSSM1; polyglucosan; glycogen synthase; glycogen; muscle; glycogen storage disease

Introduction

The ability to store glucose as the branched-chain polymer glycogen is shared by organisms as evolutionarily diverse as bacteria and mammals: it enables organisms to deal with temporary starvation by maintaining energy provision through glycogen catabolism, and, in times of plenty, to store this energy macromolecule substrate in a form that has minimal effect on cellular osmotic pressure [1]. In mammals, glycogen is normally stored in muscle and other tissues following the action of 2 key enzymes: glycogen synthase (GS) and glycogen branching enzyme (GBE). GS catalyses the polymerisation of glucose from a UDP-glucose (UDPG) substrate via α1-4 glycosidic bonds and GBE is responsible for generating α1-6 bonds, every 4-10 residues [2]. There are 2 GS isoforms: one, encoded by the *GYS1* gene and predominantly expressed in muscle but also in other tissues and the other encoded by the *GYS2* gene and expressed only in liver. Both GS isoforms are regulated by protein kinase-catalysed phosphorylation and allosteric modulation by glucose-6-phosphate (G6P) [3].

There are more than 14 glycogen storage diseases in humans and animals [4-7], several of which are characterised by excessive muscle glycogen or polyglucosan and caused by enzymatic defects in glycogenesis or glycogenolysis. In 2008, a missense, autosomal dominant mutation (R309H) in *GYS1* was identified in Quarter Horses with polysaccharide storage myopathy (PSSM1) [8], a disease characterised by intermittent exertional rhabdomyolysis episodes and excessive muscle glycogen and amylopectate accumulation [9,

10] but with an absence of cardiac signs [11]. The R309H mutation is associated with increased GS activity in muscle from affected horses [8]. The identical mutation has now been reported in many horse breeds worldwide [12-15] suggesting dissemination from a single founder and in certain breeds, positive selection [16] perhaps due to the increased muscle glycogen storage in affected animals [8]. Since the ratio of GS: GBE activity is important in the formation of glycogen with a normal structure [17], filamentous alpha crystalline polysaccharide that forms in PSSM1-affected muscle likely develops because of an increased GS: GBE activity ratio [18] as seen in transgenic mice with constitutively active muscle GS [19]. The mechanism by which the equine R309H mutation results in increased GS activity is unknown; potential mechanisms include elevated GS expression, reduced degradation or dysregulation of enzyme activity. However, since the R309H mutation occurs in a highly conserved region of all GS enzymes and a mutation of an adjacent amino acid in yeast GS (equivalent to amino acid G310 in mammalian GS) also results in increased enzyme activity [20], it is possible that mutations in this region cause constitutive enzyme activation.

Covalent regulation of GS is dependent on 9 separate phosphorylation sites that are modified by various upstream kinases; of these, phosphorylation at sites 2 (serine residue S7), 2a (S10), 3a (S641) and 3b (S645) decrease the enzyme activity more than the remaining 5 sites [21-23]. Furthermore, phosphorylation of certain sites enables sequential phosphorylation of others so that they can be functionally grouped for investigative purposes [24]. Two of the key upstream kinases responsible for marked inhibition of GS are glycogen synthase kinase 3β (GSK3β) (which phosphorylates sites 3a, 3b, 3c, and 3d) and AMP-activated protein kinase (AMPK), which phosphorylates GS at site 2. Other kinases, namely Casein Kinase 2 and Protein kinase A, are associated with phosphorylation at sites 1a, 1b and 5 which have little effect on GS activity [24]. The phosphorylation of GS has a significant effect on G6P affinity; indeed, regulation by G6P is associated with a feed-forward mechanism that causes further enzyme activation by dephosphorylation [25]. Although the R309H residue is distant in the primary sequence from any of the known phosphorylation sites, the mutation could result in an inappropriate response to phosphorylation as is seen in a yeast GS variant [20].

Although the crystal structure has not been published for any mammalian GS, the structures for a bacterial GT5 synthase (*Agrobacterium tumefaciens*) [2] and, more recently, for a yeast synthase (*Saccharomyces cerevisiae*; Gsy2p) [26] and a *Caenorhabditis elegans* synthase [27] have been solved. Yeast GS is a homo-tetrameric protein in both its basal and active states and eukaryotic GT3 synthases likely have a similar tetrameric arrangement due to their high sequence identity [26]. Since the amino acid sequence surrounding the PSSM1 R309H *GYS1* mutation is highly conserved amongst species [8] it is possible that this site might have an important (but as yet unknown) functional role [2, 28]. It is not however thought to be involved in substrate binding [2, 29] or catalytic activity [2, 20, 30].

The binding of the G6P ligand to GS is complex [26]. The structural basis for G6P allosteric activation has been revealed from analysis of high-resolution crystal structures of the homologous synthase enzyme, Gsy2p from *Saccharomyces cerevisiae*: GS has a binding pocket for the phosphate side chain of G6P that comprises 5 amino acid residues that are conserved across the GT3 family glycosyltransferases [26]. G6P binding results in a major

conformational change involving translation and rotation toward the tetramer interface of the enzyme to generate the active form [26]. Co-crystallisation of Gsy2p with maltodextrin polymers (used as analogues to detect glycogen binding sites) shows that there are at least 4 maltodextrin sites for this substrate in the enzyme's active form [31]. Only binding sites 1 and 2 are exposed in the basal form of GS [31]: these sites might be important for enabling the enzyme to remain bound to glycogen even when GS activity is reduced by phosphorylation [32].

Improved understanding of the mechanism by which the R309H mutation in equine *GYS1* leads to the mutant enzyme's increased activity might help further elucidate the functional significance of an incompletely characterised domain of this fundamentally important mammalian enzyme. Furthermore, it could prompt investigation of specific treatments for this common equine myopathy or for other related glycogenoses in humans [33]. In this work, we investigate the enzyme's regulation *in silico* via computational modelling and through biochemical analysis *in vitro* of whole muscle extracts and via recombinant expressed enzyme kinetics. We hypothesised that higher GS activity in affected horse muscles is caused by (1) higher GS expression; (2) altered GS regulation by allosteric effectors or by covalent phosphorylation; or (3) constitutive activation via a conformational structural change.

Materials and Methods

Muscle sample collection

Muscle samples were collected by open biopsy under local anaesthesia from the semimembranosus muscle of 12 homozygous normal (RR), 13 heterozygote (HR) and 4 homozygous mutant (HH) Belgian and Percheron draught horses according to ethical approval from the Institutional Animal Care and Use Committee (University of Auburn). All horses were maintained at the university research facility and were managed at pasture and fed identically. Horses were selected on the basis of age- and sex-matching of individuals of differing genotype, following genotyping of the entire herd of horses using an established restriction fragment polymorphism assay [8]. Samples were snap-frozen in liquid nitrogen, shipped on dry ice and stored at −80°C until use.

Glycogen content measurement

Total glycogen was measured in 50 mg wet weight muscle biopsy samples using a colorimetric assay [34] (RR=7, RH=8, HH=4).

GS activity

GS activity was measured using radiolabelled UDP-glucose [35] in the presence of low (0.02 mM), medium (0.17 mM) and high (8 mM) G6P concentrations. Calculation of the fractional velocity of the enzyme, %FV (100 × [activity (0.17 mM G6P)/activity (8 mM G6P)]) enables investigation of the regulation of GS by G6P. Calculation of G6P-independent activity, % I-form (100 × [activity (0.02 mM G6P)/activity (8 mM G6P)]) enables investigation of GS regulation by phosphorylation [35-37].

Briefly, 20 μg of homogenised muscle (RR n=12, RH n=13, HH n=4) was placed into wells of a 96 well plate (Nunc) in duplicate and 40 μl of each of 3 different glucose concentration (final glucose concentrations: 0.02 mM, 0.17 mM or 8 mM) reagents were added. Samples were incubated with the glucose reagent (containing differing G6P concentrations, 25 mM Tris-HCl, 5 mM ethylene-diamine-tetra-acetic acid (EDTA), 10 mg/ml glycogen, 50 mM NaF, 2.5 mM unlabelled UDPG and 50 μl/ml UDPG (^{14}C)) for 25 minutes at 37°C and then 50 μl of the mixture was added to wells of Unifilter 96 well plates (Whatman) containing 200 μl 66% ice-cold ethanol in dd$H_2$0 water. The plates were then incubated at −20°C for 2h and subsequently washed in ice-cold 66% ethanol 5 times. Plates were then dried for 15 minutes at 37°C and 75 μl of Microscint 40 scintillation fluid (Perkin Elmer) was added to each well before counting using a top-count NXT scintillation counter (Perkin Elmer).

Muscle homogenisation

For measurement of total GS expression, skeletal muscle homogenates were prepared from 50 mg of snap frozen biopsy tissue dissected free of any visible fat or connective tissue and crushed using a pestle and mortar cooled using dry-ice. The powder was then dissolved in 1 ml of protein extraction buffer containing phosphatase inhibitors, heated at 100°C for 5 minutes and subsequently centrifuged (16000g for 5 minutes at 4°C). The supernatant was removed and its protein concentration measured using the Pierce BCA protein assay.

A modified extraction was performed on skeletal muscle homogenates for measurement of phosphorylated isoforms of GS and upstream kinases. 40 mg of frozen muscle was cut into small pieces and submerged in 600 μl of protein extraction buffer, before homogenising using a Qiagen TissueLyser (2 × 30 seconds at 30000 Hz). The samples were then rotated end over end for 1 h at 4°C and protein concentration was then determined as above.

Total glycogen synthase expression

Whole muscle protein homogenates were separated using 8% acrylamide gels and transferred onto nitrocellulose membranes (Amersham). Total GS expression was measured using a rabbit monoclonal antibody to the C-terminus of human GS (Clone EP817Y; Epitomics; 1: 10000) and membranes were co-blotted with a mouse monoclonal antibody to human desmin (Clone D33, Dako; 1: 50000). Secondary antibodies were HRP-conjugated goat antibodies (either anti-rabbit or anti-mouse; BioRad; 1:5000). All antibodies were incubated for 1 hour at room temperature. Chemiluminescence was measured with the ECL-prime kit (Amersham) and Amersham Hyperfilm ECL (GE Healthcare). Assay linearity was confirmed with pilot experiments via loading of increasing amounts of protein per lane (results not shown). Films were digitised using a Stylus Photo RX640 printer and scanner (Epson, Hemel Hempstead, UK) alongside a 21-step transmission step wedge (Stouffer Graphic Arts, Mishawaka, USA). The mean grey intensity values from equal rectangular areas of each region of the step wedge were quantified in ImageJ (NIH, Bethesda, USA). Total GS expression was calculated as a ratio to desmin expression to control for loading.

Phosphorylated GS isoform expression

Muscle protein samples were separated using 8% self cast acrylamide gels and then transferred using a semi-dry technique (Amersham TE77) onto a PVDF membrane

(Millipore). Sheep polyclonal primary antibodies were those used previously against phosphorylation epitopes of sites 1b (2μg/ml), 2+2a (4μg/ml) and 3a+3b (1μg/ml) of GS [35, 38]. Appropriate HRP-conjugated secondary antibodies were used (Dako; 1:5000). All antibodies were incubated for 1 hour at room temperature. Chemiluminesence was measured using Luminata Forte HRP chemiluminescent subrstrate (Millipore). After quantification using ImageLab software (Biorad), membranes were stripped of antibodies and then re-incubated with a total GS antibody as previously described. Results are presented as a ratio of the phosphorylated enzyme to total GS expression.

GLUT4, GSK3β and AMPK phosphorylation and expression

Using the same technique as for phosphorylated isoforms of GS, total GLUT4 (Pierce; 1:1000), total GSK3β D transduction Laboratories; 1:500), phosphorylated GSK3β (Cell Signalling; 1:1000) and AMPK (α1; 1:5000, α2; 1:15000 and β1; 1:1000, as described by Woods et al. [39], β2:1:3000, as described by Durante et al. [40] and pAMPK Thr172; 1:1000 from Cell Signalling) protein expression levels were measured in whole muscle homogenates. Antibodies directed against the AMPK γ1 and γ3 subunits did not detect the equine protein. All primary antibodies were diluted in 2% skimmed milk and incubated overnight at 4°C and all secondary antibodies were incubated for 45 minutes at room temperature. Appropriate HRP-conjugated secondary antibodies were used (Jackson IR; 0.16μg/ml for pGSK3β. Dako; 1:5000 for all others). GLUT4 and total GSK3β expression were quantified in muscle protein samples using α-actin (Sigma; 1:8000) as a loading control. Phosphorylated GSK3β was expressed as a ratio to total GSK3β expression. AMPK expression was calculated and normalised according to a standard curve derived from protein homogenates of known quantities as is custom for this assay [41]. Chemiluminesence was measured using Luminata Forte HRP chemiluminescent substrate (Millipore) and quantified using ImageLab software (BioRad).

GS baculovirus cloning and expression

Full-length amplicons of R309 wild-type and H309 mutant *GYS1* cDNAs, obtained from homozygous wild-type and homozygous mutant muscle RNA respectively, were cloned into the PH promoter of the pFastBac dual vector (Invitrogen) between the BamH1 and Xba1 cloning sites. Subsequently, a full-length amplicon of equine glycogenin (GYG1) cDNA was subcloned into the p10 promoter of both the wild-type R309 GS*pFastBac and the H309 mutant Gs*pFastbacs between the Nhe1 and Xho1 cloning sites, allowing co-expression of active equine GS with equine glycogenin in *Spodoptera frugiperda* Sf9 insect cells. Each of the cloned insert sequences in each vector was verified with Sanger sequencing. Western blot of harvested insect cells from each of 3 different clones of mutant and wild type vectors was then used to confirm the expression of wild-type GS and R309H GS together with glycogenin. Large culture volumes of these cells (1 litre) were grown and cell pellets harvested by Kinnakeet Biotechnology, USA.

Purification of recombinant horse glycogen synthase

The insect cell pellets were resuspended and lysed in 50 ml of extraction buffer containing 50 mM Tris-HCl, pH 7.8, 300 mM NaCl, 0.1% Triton X-100, 2 mM EDTA, 1 mM benzamidine, 0.5 mM phenylmethanesulfonyl fluoride (PMSF), 10 mM β-mercaptoethanol

(BME). The crude cell extracts were centrifuged at 35,000 rpm in a Beckman Ti-45 rotor for 30 minutes at 4°C and the supernatants were collected. Ethanol (kept at −80°C prior to use) was slowly added to the clarified cell lysates, under constant stirring, to a final concentration of 30%. This process was done in an ice/salt broth so that the temperature stayed between −1 and −5° C, ensuring complete precipitation of the endogenous insect cell glycogen (no additional glycogen was added). The suspensions were then centrifuged at 9000g for 60 min at −3°C. The supernatant was discarded and the glycogen pellets were resuspended in 100 ml of loading buffer containing 50 mM Tris-HCl, 300 mM NaCl, 1 mM benzamidine, 0.5 mM PMSF and 2 mM BME. The resuspended pellets were then loaded onto a Concanavalin-A (Sigma) column. After washing the column with 20 column volumes of loading buffer, the protein was gradient eluted with glucose (0-400 mM). The fractions that had GS activity (in the presence of 10 mM G6P) were pooled and then dialysed extensively against a buffer containing 50 mM Tris-HCl, 300 mM NaCl and 2 mM BME to remove the free glucose. The protein was then concentrated and mixed with glycerol to a final concentration of 35% and stored at −20° C for long term usage [42].

Specific activity and activity ratio measurement

GS activity was measured in the recombinant enzymes by the method of Thomas *et al.* which quantifies the amount of ^{14}C-glucose transferred from ^{14}C-labelled UDP-glucose to glycogen over a period of 15 min at 30°C [43]. Standard reaction conditions used 4.44mM UDP-glucose and 6.67 mg/ml of glycogen. Prior to use, rabbit liver glycogen type-III was deionised by passing it through TMD-8 hydrogen and hydroxide form-mixed bed exchanger resins. Activity was measured both in the presence or absence of 10 mM G6P and before and after treatment with 50μg/ml recombinant protein phosphatase 1 (PP1) (gamma) (gift of Dr. Anna DePaoli-Roach, Indiana University), the latter in comparison with similarly treated recombinant WT and mutant (S7A) human GS (description of S7A mutant given in supplementary methods). In order to dephosphorylate phosphorylated serine, threonine and tyrosine residues, 50 μg of different GS samples were incubated with 50 μg of PP1 gamma catalytic subunit 1, at 30°C for 30 minutes. The reaction mix also contained 0.2mM $MnCl_2$ which is essential for protein phosphatase 1 activity. After 30 minutes, GS reaction mix was added (containing 4.44mM UDP-glucose, 6.67 mg/ml of glycogen, C^{14} UDP-glucose, 1mM 1,4-dithiothreitol (DTT) and 1mM EDTA (final concentrations)). The EDTA present in the GS reaction mix will terminate the phosphatase reaction. The activity ratio is the ratio of the activity in the absence of G6P to the activity in the presence of 10 mM or 7.2mM G6P (muscle or insect extracts respectively). Protein concentration was measured by Bradford's method, using bovine serum albumin as a standard.

Enzyme kinetics for UDP-Glucose and Glucose-6-Phosphate

For the UDP-glucose titrations, 7 different concentrations of UDPG (0.1 mM to 15 mM for the wild type (WT) enzyme and 0.05 mM to 6 mM for the mutant R309H enzyme) were used, keeping the glycogen concentration constant at 6.67 mg/ml either in the presence or absence of 10 mM G6P. Eight different concentrations of G6P (0.1mM to 20mM for the WT enzyme and 0.05mM to 10mM for the mutant R309H enzyme) were used for the G6P titrations under standard reaction conditions.

Kinetic data analysis

The enzyme kinetic data were analyzed using SigmaPlot (v12.3). The activation curves for G6P were fitted to the 4 parameter logistic curve and the $S_{0.5}$ values were obtained from these fits. The substrate saturation curves were fitted to the standard Michaelis-Menten equation $v=V_{max}*[S]/(K_m+[S])$, where v is the reaction rate, [S] is the substrate concentration, V_{max} is the maximum rate achieved by the system and K_m is the substrate concentration at half maximum velocity. The V_{max} and K_m values were obtained from these fits and the results represent the mean of 3 separate experiments.

Insect protein site 3a phosphorylation

100ng samples of different GS proteins (as used for kinetic studies) were separated by 10% SDS-PAGE and transferred onto a 0.45-μm nitrocellulose membrane (Bio-Rad) at 30 V, overnight. After transfer, the membranes were blocked in 5% nonfat milk powder in 1X Tris-buffered saline (TBS) containing 0.1% Tween 20. The membrane was then incubated overnight at 4° C with phospho 3a (Ser641) specific rabbit GS primary antibody obtained from Cell Signaling (3891). The membranes were then washed and subsequently incubated with horseradish peroxidase-conjugated secondary antibodies (Cell Signaling, 7074) for 5 h at room temperature. Detection was performed by enhanced chemiluminescence using Pierce ECL western blot substrate purchased from Thermo Scientific. After detection, the membranes were treated with stripping buffer containing 62.5 mM Tris-HCl, pH 6.8, 2% sodium dodecyl sulfate, 0.7% β-mercaptoethanol to remove the phospho 3a primary and secondary antibodies. After stripping, the same membranes were incubated overnight at 4° C with rabbit GS specific primary antibodies (Cell Signaling, 3886). The membranes were then washed, treated with secondary antibodies and developed as described above. In all cases, prior to use, the primary and secondary antibodies were diluted 1:2000 and 1:4000, respectively. Densitometric analysis of the immunoblots was performed using Quantity One software package.

Homology modelling

X-ray crystal structures of *S. cerevisiae* Gsy2p in the basal state (PDB code 3NAZ; 3 Å resolution) and G6P bound state (PDB code 3NB0; 2.41 Å resolution) provided the templates for homology modelling of equine GS. The full-length sequence of equine GS was retrieved from Genbank (accession ACB14276) and sequence aligned with *S. cerevisiae* Gsy2p using Clustal Omega [44]. MODELLER software [45] was used to generate 50 models of both the basal and bound tetrameric forms of equine GS. In both cases the internal scoring function of MODELLER was used to select 10 models that were visually inspected and submitted to the VADAR webserver [46] for assessment of stereochemical soundness in order to select a single best model. The R309H mutation was introduced into both models using SwissPDBViewer [47]. Model figures were generated using PyMOL (DeLano Scientific, San Carlos, CA, U.S.A.).

Statistical analysis

Data calculations and statistical analysis were performed using GraphPad Prism (Version 6.0). Due to the small sample size for the homozygous mutant group, non-parametric

statistics were performed and statistical significance was assessed via a Kruskal-Wallis test and Dunn's post-hoc multiple comparison test. Results were considered statistically significant when $P<0.05$. Pearson's correlation was used to examine association between continuous variables.

Results

Breed and signalment data

There were no significant differences in age, sex or breed of the 3 genotyped groups used for this study (Table S1).

Muscle glycogen content, GS activity and total GS expression

Heterozygote (RH) and homozygote (HH) mutant horses had significantly higher glycogen content in skeletal muscle than control (RR) horses (Figure 1A), despite there being no difference in total muscle GS expression between each of the genotyped groups ($p=0.98$) (Figure 1B). The higher glycogen content of mutant horse muscle was accompanied by higher GS activity in muscle samples from homozygotes (HH) compared to samples from heterozygotes and between homozygotes (HH) and WT controls (RR) in the presence (Figure 1C, %FV, $p=0.03$) and the absence of G6P (Figure 1D, %I-form, $p=0.04$) but there was no difference in maximal GS enzyme activity between genotypes ($p=0.20$, data not shown).

Phosphorylation of GS

PSSM1-homozygote muscle samples had greater phosphorylation at site 2+2a than WT samples (Figure 2B; $p=0.009$). There were no detectable differences in levels of GS phosphorylation at the other target sites (1b and 3a+3b) between the genotypes (Figure 2A and 2C).

GS activity is dependent on its phosphorylation; in particular, phosphorylation of sites 3a, 3b and 2+2a and is highly dependent on glycogen content via negative feedback [35]. Due to the significant increase in phosphorylation at sites 2+2a, correlation coefficients were calculated between site 2+2a phosphorylation and glycogen content and GS activity. Muscle glycogen content was significantly, but weakly correlated with the degree of GS site 2+2a GS phosphorylation ($R^2=0.23$, $p=0.04$); there was no significant association between phosphorylation at site 2+2a and GS activity (data from whole cohort; $p=0.54$).

GLUT4, GSK3β and AMPK expression

There was no difference in expression of GLUT4 ($p=0.42$), total GSK3β ($p=0.49$) or in the ratio of phosphorylated GSK3β (Ser9) to total GSK3β ($p=0.43$) between different genotypes (data not shown). However, there was significantly higher expression of AMPKα1 protein in the PSSM1-homozygote samples compared to WT controls (Figure 3A; $p=0.04$) and a trend towards elevated phosphorylation of AMPK (pAMPK) in PSSM1-homozygote muscle samples compared to WT and heterozygotes (Figure 3E), although this did not reach significance ($p=0.13$). There was a significant and strong association between AMPKα1 expression and pAMPK (Figure 3F; $R^2=0.66$, $p<0.0001$). There was also

significantly lower AMPKβ1 expression in PSSM1-homozygote samples compared to heterozygotes (Figure 3C; p=0.03) but not compared to WT controls.

Kinetics of expressed and purified GS

WT and mutant equine GS were expressed in insect cells and the purified enzymes were used to compare kinetic parameters, including dependence on G6P concentration, the K_m for UDPG and V_{max} in the presence and absence of G6P, the V_{max}/K_m ratios with and without G6P, and the $S_{0.5}$ for G6P in the presence of 4.4 mM UDPG.

The G6P titration curves for the WT and the R309H mutant enzymes show that the activity of both enzymes increased with increasing G6P concentrations and that the mutant enzyme is nearly maximally activated at G6P concentrations that barely activate the WT enzyme (Figure 4A). Specifically, G6P activated both the WT and mutant enzymes with an $S_{0.5}$ value of around 3.0 mM and 0.24 mM respectively (Table 1).

GS activity measurements performed at varying UDPG concentrations (Figure 4B), in the absence and presence of maximal (10 mM) G6P, revealed that the mutant enzyme had a much lower K_m for UDPG (0.48 and 0.18 mM, with and without G6P, respectively) than the WT enzyme (2.4 and 1.6 mM, with and without G6P, respectively (Table 1). The V_{max}/K_m ratios with and without G6P were also much higher for the mutant when compared to the WT GS (Table 1).

The R309H mutant enzyme shows an approximately 20 fold higher activity ratio than the WT enzyme (Table 2), due largely to the mutant enzyme's marked activation in the absence of G6P. The low activity ratio seen in the WT equine GS enzyme (0.02) is similar to that detectable in baculovirus-generated human GS [48]. Despite both the equine WT and mutant insect-derived enzymes' phosphorylation (at site 3a) (Figure 5A), the mutant equine enzyme had a high activity ratio, similar to that of the S7A mutant human GS, (which cannot be phosphorylated) (Figure 5B). Phosphatase treatment induced a marked increase in the activity ratio of both the WT equine and human GS enzymes from minimal baseline ratios as expected; in contrast, there was little change in the activity ratio of WT equine enzyme which behaved similarly to the S7A mutant human enzyme (Figure 5B).

Glycogen synthase homology modelling

The residues resolved in the G6P-bound crystal structure of yeast Gsy2p and the corresponding region of equine GS share 55% sequence overall identity (Figure 6). Conserved residues include the binding determinants of G6P and maltodextrin. In addition, the R309 residue and the 5 surrounding residues of equine GS are conserved as R298 in yeast Gsy2p (Figure 6). Therefore Gsy2p structures with and without G6P bound, provided suitable structural templates for homology modelling of equine GS as a homotetramer with basal and active conformations, respectively (Figure 7A and B).

As a first step in understanding the structural effects of the R309H mutation, the environment around R309 was inspected in the WT GS models. In both basal and active GS models, R309 is distal from the G6P and maltodextrin binding sites (Figure 7A and B) and is therefore not predicted to form a direct binding contact for either substrate. Nevertheless,

R309 is located on the C-terminal end of an α-helix that contains 4 residues (H291, Q294, H297, K301) that are G6P binding determinants. In addition, R309 is positioned adjacent to a pair of α-helices that use a coiled-coil interaction to form the major interface between subunits of the tetramer. Indeed, conformational transition between basal and active states involves translation and rotation around this central tetrameric interface [26] (Figure 7A and B).

R309 in the GS models and the corresponding R298 residue in the yeast Gsy2p structures have similar interactions (Figure 7C-H). Gsy2p R298 forms a salt bridge with the side chains of D295 in the basal state (Figure 7G). This interaction is lost in the active state (Figure 7H) and, whereas R298 forms no new interactions, its former interaction partner, D295, instead forms a salt bridge with residue R376. R376 is located on the adjacent α-helix that forms the aforementioned coiled-coil configuration of the enzyme subunit interface. A similar state-dependent switch in salt bridges is found with equine WT GS. R309 engages in a salt bridge with E306 and, as with Gsy2P, this interaction is lost in the active state where E306 is instead available to form a salt bridge with K387.

The R309H mutation was introduced into GS models and the predicted outcome was the elimination of the salt bridge interaction with E306 in the basal-state conformation (Figure 7E). Release of E306 from an interaction with the 309 position may instead allow it to interact with the adjacent K387 even in mutant enzyme's basal state.

Discussion

The inherited skeletal muscle disorder known as PSSM1, caused by a missense mutation in the equine *GYS1* gene [8] is histopathologically characterised by increased amylopectate and glycogen in skeletal muscle fibres [9, 10]. Here, we employed a multi-disciplinary approach in order to determine if the basis for the previously-identified, increased GS activity in PSSM1-affected muscle [8] is associated with altered GS enzyme expression, dysregulation of GS activity, or a GS protein conformational change with possible constitutive activation. Our results reveal that the R309H mutation, responsible for this highly prevalent equine polyglucosan myopathy, present in over 20 breeds worldwide [12-15], is caused by constitutive activation; furthermore, we propose the probable mechanism, based on modelling analyses of the mutant GS structure.

Similar to previous results in Quarter Horses, (a PSSM1-affected light horse breed) [49], we have shown that mutant draught horses with the same mutation have increased muscle glycogen storage despite normal GLUT4 transporter expression. Homozygous mutant muscle had increased GS activity compared to homozygous WT muscle, even though there was no difference in total GS expression between genotypes. GS in skeletal muscle from homozygous mutant horses had increased G6P-independent activity (%I-form), consistent with data from McCue *et al.,* who detected higher GS activity, irrespective of G6P concentration, in PSSM1-affected Quarter Horses [8]. Despite the differences between PSSM1-homozygotes and PSSM1-heterozygotes in terms of muscle GS activity, there was no difference between these groups in the glycogen content of their muscle, but the reason is unclear. As GS activity is inversely correlated with the extent of site 2+2a GS

phosphorylation in healthy muscle [35, 38, 50], the higher enzyme activity in mutant horses cannot be explained by inappropriate (i.e. reduced) GS phosphorylation, since muscle from affected horses actually had significantly more GS phosphorylation at site 2+2a, (and no difference in phosphorylation at other evaluated sites) when compared with controls. As expected in healthy muscle [36], PSSM1-affected horses had increased phosphorylation at site 2+2a in the presence of elevated muscle glycogen, most likely reflecting a normal physiological attempt to reduce enzyme activity [35, 50-52]; indeed, the high GS activity in mutant horses occurs despite the phosphorylation and increased expression of AMPK, the principal upstream kinase for phosphorylation at site 2. Therefore, phosphorylation of the mutant enzyme at site 2+2a does not correspondingly lower its activity.

The increased activity detectable in PSSM1-horse muscle most likely results from a constitutive change in the mutant enzyme's function, similar to that of a yeast mutant that also fails to respond appropriately to phosphorylation [8, 20] or to increased glycogen content [53]. In order to test this hypothesis, enzyme kinetic studies were performed using purified protein extracts derived from allele-specific GS, expressed in insect cells. These analyses revealed that the mutant enzyme behaves as if it is nearly fully active even in the absence of its allosteric activator, G6P as is shown by the significantly lower K_m and increased V_{max} in the absence of G6P. Further, the R309H enzyme had significantly lower K_m for UDPG even in the absence of G6P and the V_{max}/K_m value for the mutant enzyme in the absence of G6P was increased over 60 fold, when compared to the WT enzyme. In contrast, the activity ratio of the WT equine enzyme was similar to that of human GS purified in a similar manner [48]. Further, there was no detectable difference in the extent of 3a phosphorylation between the WT and mutant recombinant enzymes, but despite this, the equine recombinant enzyme behaved similarly to that of a mutant human enzyme that cannot be phosphorylated, both with and without pre-treatment with protein phosphatase 1. Our data therefore confirm that the R309H mutation associated with PSSM1 is a true, gain of function mutation.

The phosphorylation sites of muscle GS are located on the N- and C- termini of the enzyme [54, 55]. We were unable to use homology modelling to investigate these sites as there are no corresponding regions resolved in the yeast Gsy2p structures. Nevertheless, the region around R309 was modelled (Figure 7) and, although not predicted to form a binding contact for G6P or maltodextrin (Figure 7A and B), this residue is positioned at a pivotal position near the tetrameric interface of the enzyme and is located on an α-helix that harbours 4 G6P binding residues. Therefore, a structural perturbation at the 309 position could influence the position of the conformational equilibrium making it easier to adopt the active conformation. Modelling indicates that in the enzyme's basal state, R309 normally engages in a salt bridge with E306 whereas in the active state, E306 forms an alternative salt bridge with K387 (Figure 7C and D). These salt bridge interactions might be important for stabilising the conformation of their respective functional states. We therefore propose that the R309H mutation, which is predicted to eliminate the basal-state salt bridge (Figure 7E), likely shifts the conformational equilibrium of the enzyme to the active state and reduces its tendency to adopt an inhibited state (Figure 7F). Interestingly, the residue adjacent to R309 is conserved as a glycine in both equine GS (G310) and in yeast Gsy2p (G299) where its mutation results in increased Gsy2p activity [20]. This glycine is located at a turn at the C-terminal end of the

helix containing R298 (equivalent to equine R309) and G6P binding contacts. It is therefore positioned to function as a typical glycine-hinge residue and the reported mutation-associated change in enzyme activity [15], provides further evidence that structural deviations in this region produce constitutive activation.

In summary, our work provides further evidence that the PSSM1-associated R309H *GYS1* mutation results in increased glycogen content and GS activity in skeletal muscle. We show that this elevated activity results in an altered sensitivity to G6P, increased affinity for UDPG and occurs despite hyperphosphorylation at site 2+2a and increased expression of AMPK. Further, for the first time, we suggest through predictive modelling a potential mechanism by which this occurs. Additional work is needed to explain all the phenotypic features of this equine disorder, including the intermittent rhabdomyolysis and gait abnormalities seen in some affected horses. ATP depletion is a common cause of rhabdomyolysis in humans and therefore further work investigating metabolic responses in affected horses might help explain some aspects of the clinical phenotypes in this disorder. However, our results suggest that therapeutic modification of AMPK activity might be ineffective in mutant animals, as increased GS phosphorylation does not reduce the mutant enzyme's hyperactivity; instead, efforts aimed at direct enzyme inhibition might be more effective. Finally, dysregulation of GS or other related enzymes should be considered in humans and animals with glycogen storage diseases of unknown origin, particularly when a dominant mode of inheritance is identified; indeed, this common equine disease represents a large animal model for evaluation of treatments aimed at reducing polyglucosan formation in skeletal muscle [33], a feature of a number of important, but comparatively rare, human myopathic disorders.

Supplementary Material

Refer to Web version on PubMed Central for supplementary material.

Acknowledgements

We thank the staff at Auburn University for providing the muscle samples for this work, Professor Bonnie Wallace at Birkbeck University for her advice on homology modelling and Dr James Ervasti at the University of Minnesota for expert advice and guidance on the baculovirus expression system.

Declaration of funding and conflict of interest

This work was partly funded by The Petplan Charitable Trust (Award S12-25), The Morris Animal Foundation (Award D14EQ-404) awarded to RJ Piercy and C Maile and by the National Institutes of Health, National Institute of Arthritis, Musculoskeletal and Skin Diseases award 1K08AR055713-01A2 to ME McCue. TD Hurley and KK Mahalingan were supported by NIH grant R01-79887. JFP Wojtaszewski and JR Hingst were supported by the Danish Council for Independent Research and the Ministry of Culture. This manuscript was approved by The Royal Veterinary College's Research Office (reference number: CSS_00938).

References

1. Wilson WA, et al. Regulation of glycogen metabolism in yeast and bacteria. FEMS Microbiol Rev. 2010; 34(6):952–85. [PubMed: 20412306]
2. Buschiazzo A, et al. Crystal structure of glycogen synthase: homologous enzymes catalyze glycogen synthesis and degradation. Embo J. 2004; 23(16):3196–205. [PubMed: 15272305]

3. Jensen J, Lai YC. Regulation of muscle glycogen synthase phosphorylation and kinetic properties by insulin, exercise, adrenaline and role in insulin resistance. Arch Physiol Biochem. 2009; 115(1): 13–21. [PubMed: 19267278]

4. Gregory BL, et al. Glycogen storage disease type IIIa in curly-coated retrievers. J Vet Intern Med. 2007; 21(1):40–6. [PubMed: 17338148]

5. Lohi H, et al. Expanded repeat in canine epilepsy. Science. 2005; 307(5706):81. [PubMed: 15637270]

6. Ozen H. Glycogen storage diseases: new perspectives. World J Gastroenterol. 2007; 13(18):2541–53. [PubMed: 17552001]

7. Fyfe JC, et al. Glycogen storage disease type IV: inherited deficiency of branching enzyme activity in cats. Pediatr Res. 1992; 32(6):719–25. [PubMed: 1337588]

8. McCue ME, et al. Glycogen synthase (GYS1) mutation causes a novel skeletal muscle glycogenosis. Genomics. 2008; 91(5):458–66. [PubMed: 18358695]

9. Valberg SJ, et al. Polysaccharide storage myopathy associated with recurrent exertional rhabdomyolysis in horses. Neuromuscul Disord. 1992; 2(5-6):351–9. [PubMed: 1284408]

10. Naylor RJ, et al. Allele copy number and underlying pathology are associated with subclinical severity in equine type 1 polysaccharide storage myopathy (PSSM1). PLoS One. 2012; 7(7):e42317. [PubMed: 22860112]

11. Naylor RJ, et al. Evaluation of cardiac phenotype in horses with type 1 polysaccharide storage myopathy. J Vet Intern Med. 2012; 26(6):1464–9. [PubMed: 22978303]

12. Stanley RL, et al. A glycogen synthase 1 mutation associated with equine polysaccharide storage myopathy and exertional rhabdomyolysis occurs in a variety of UK breeds. Equine Vet J. 2009; 41(6):597–601. [PubMed: 19803057]

13. Herszberg B, et al. A GYS1 gene mutation is highly associated with polysaccharide storage myopathy in Cob Normand draught horses. Anim Genet. 2009; 40(1):94–6. [PubMed: 18822097]

14. Schwarz B, et al. Estimated prevalence of the GYS-1 mutation in healthy Austrian Haflingers. Vet Rec. 2011; 169(22):583. [PubMed: 21949056]

15. Johlig L, et al. Epidemiological and genetic study of exertional rhabdomyolysis in a Warmblood horse family in Switzerland. Equine Vet J. 2011; 43(2):240–5. [PubMed: 21592222]

16. McCoy AM, et al. Evidence of positive selection for a glycogen synthase (GYS1) mutation in domestic horse populations. J Hered. 2014; 105(2):163–72. [PubMed: 24215078]

17. Pederson BA, et al. Overexpression of glycogen synthase in mouse muscle results in less branched glycogen. Biochem Biophys Res Commun. 2003; 305(4):826–30. [PubMed: 12767905]

18. Valberg SJ, et al. Glycogen branching enzyme deficiency in quarter horse foals. J Vet Intern Med. 2001; 15(6):572–80. [PubMed: 11817063]

19. Raben N, et al. Surprises of genetic engineering: a possible model of polyglucosan body disease. Neurology. 2001; 56(12):1739–45. [PubMed: 11425943]

20. Anderson C, Tatchell K. Hyperactive glycogen synthase mutants of Saccharomyces cerevisiae suppress the glc7-1 protein phosphatase mutant. J Bacteriol. 2001; 183(3):821–9. [PubMed: 11208778]

21. Prats C, et al. Phosphorylation-dependent translocation of glycogen synthase to a novel structure during glycogen resynthesis. J Biol Chem. 2005; 280(24):23165–72. [PubMed: 15840572]

22. Roach PJ. Glycogen and its metabolism. Curr Mol Med. 2002; 2(2):101–20. [PubMed: 11949930]

23. Skurat AV, Wang Y, Roach PJ. Rabbit skeletal muscle glycogen synthase expressed in COS cells. Identification of regulatory phosphorylation sites. J Biol Chem. 1994; 269(41):25534–42. [PubMed: 7929255]

24. Roach PJ. Control of glycogen synthase by hierarchal protein phosphorylation. FASEB J. 1990; 4(12):2961–8. [PubMed: 2168324]

25. Bouskila M, et al. Allosteric regulation of glycogen synthase controls glycogen synthesis in muscle. Cell Metab. 2010; 12(5):456–66. [PubMed: 21035757]

26. Baskaran S, et al. Structural basis for glucose-6-phosphate activation of glycogen synthase. Proc Natl Acad Sci U S A. 2010; 107(41):17563–8. [PubMed: 20876143]

27. Zeqiraj E, et al. Structural basis for the recruitment of glycogen synthase by glycogenin. Proc Natl Acad Sci U S A. 2014; 111(28):E2831–40. [PubMed: 24982189]
28. Landau M, et al. ConSurf 2005: the projection of evolutionary conservation scores of residues on protein structures. Nucleic Acids Res. 2005; 33(Web Server issue):W299–302. [PubMed: 15980475]
29. Pederson BA, et al. Regulation of glycogen synthase. Identification of residues involved in regulation by the allosteric ligand glucose-6-P and by phosphorylation. J Biol Chem. 2000; 275(36):27753–61. [PubMed: 10874034]
30. Furukawa K, et al. Identification of Lys277 at the active site of Escherichia coli glycogen synthase. Application of affinity labeling combined with site-directed mutagenesis. J Biol Chem. 1994; 269(2):868–71. [PubMed: 8288640]
31. Baskaran S, et al. Multiple glycogen-binding sites in eukaryotic glycogen synthase are required for high catalytic efficiency toward glycogen. J Biol Chem. 2011; 286(39):33999–4006. [PubMed: 21835915]
32. Suzuki Y, et al. Insulin control of glycogen metabolism in knockout mice lacking the muscle-specific protein phosphatase PP1G/RGL. Mol Cell Biol. 2001; 21(8):2683–94. [PubMed: 11283248]
33. Hedberg-Oldfors C, Oldfors A. Polyglucosan storage myopathies. Mol Aspects Med. 2015; 46:85–100. [PubMed: 26278982]
34. Chan TM, Exton JH. A rapid method for the determination of glycogen content and radioactivity in small quantities of tissue or isolated hepatocytes. Anal Biochem. 1976; 71(1):96–105. [PubMed: 1275237]
35. Prats C, et al. Dual regulation of muscle glycogen synthase during exercise by activation and compartmentalization. J Biol Chem. 2009; 284(23):15692–700. [PubMed: 19339242]
36. Jensen J, et al. Muscle glycogen inharmoniously regulates glycogen synthase activity, glucose uptake, and proximal insulin signaling. Am J Physiol Endocrinol Metab. 2006; 290(1):E154–E162. [PubMed: 16118249]
37. Jensen J, et al. Improved insulin-stimulated glucose uptake and glycogen synthase activation in rat skeletal muscles after adrenaline infusion: role of glycogen content and PKB phosphorylation. Acta Physiol Scand. 2005; 184(2):121–30. [PubMed: 15916672]
38. Hojlund K, et al. Increased phosphorylation of skeletal muscle glycogen synthase at NH2-terminal sites during physiological hyperinsulinemia in type 2 diabetes. Diabetes. 2003; 52(6):1393–402. [PubMed: 12765949]
39. Woods A, et al. The alpha1 and alpha2 isoforms of the AMP-activated protein kinase have similar activities in rat liver but exhibit differences in substrate specificity in vitro. FEBS Lett. 1996; 397(2-3):347–51. [PubMed: 8955377]
40. Durante PE, et al. Effects of endurance training on activity and expression of AMP-activated protein kinase isoforms in rat muscles. Am J Physiol Endocrinol Metab. 2002; 283(1):E178–86. [PubMed: 12067859]
41. Højlund K, et al. AMPK activity and isoform protein expression are similar in muscle of obese subjects with and without type 2 diabetes. Am J Physiol Endocrinol Metab. 2004; 286(2):E239–44. [PubMed: 14532170]
42. Zhang W, DePaoli-Roach AA, Roach PJ. Mechanisms of multisite phosphorylation and inactivation of rabbit muscle glycogen synthase. Arch Biochem Biophys. 1993; 304(1):219–25. [PubMed: 8391782]
43. Thomas JA, Schlender KK, Larner J. A rapid filter paper assay for UDPglucoseglycogen glucosyltransferase, including an improved biosynthesis of UDP-14C-glucose. Anal Biochem. 1968; 25(1):486–99. [PubMed: 5704765]
44. Sievers F, et al. Fast, scalable generation of high-quality protein multiple sequence alignments using Clustal Omega. Mol Syst Biol. 2011; 7:539. [PubMed: 21988835]
45. Eswar N, et al. Comparative protein structure modeling using MODELLER. Curr Protoc Protein Sci. 2007 Chapter 2: p. Unit 2.9.
46. Willard L, et al. VADAR: a web server for quantitative evaluation of protein structure quality. Nucleic Acids Res. 2003; 31(13):3316–9. [PubMed: 12824316]

47. Guex N, Diemand A, Peitsch MC. Protein modelling for all. Trends Biochem Sci. 1999; 24(9): 364–7. [PubMed: 10470037]

48. Khanna M, et al. Expression and purification of functional human glycogen synthase-1 (hGYS1) in insect cells. Protein Expr Purif. 2013; 90(2):78–83. [PubMed: 23711380]

49. Annandale EJ, et al. Insulin sensitivity and skeletal muscle glucose transport in horses with equine polysaccharide storage myopathy. Neuromuscul Disord. 2004; 14(10):666–74. [PubMed: 15351424]

50. Hojlund K, et al. Dysregulation of glycogen synthase COOH- and NH2-terminal phosphorylation by insulin in obesity and type 2 diabetes mellitus. J Clin Endocrinol Metab. 2009; 94(11):4547–56. [PubMed: 19837931]

51. Jorgensen SB, et al. The alpha2-5'AMP-activated protein kinase is a site 2 glycogen synthase kinase in skeletal muscle and is responsive to glucose loading. Diabetes. 2004; 53(12):3074–81. [PubMed: 15561936]

52. Wojtaszewski JF, et al. Glycogen-dependent effects of 5-aminoimidazole-4-carboxamide (AICA)-riboside on AMP-activated protein kinase and glycogen synthase activities in rat skeletal muscle. Diabetes. 2002; 51(2):284–92. [PubMed: 11812734]

53. Lai YC, et al. Glycogen content and contraction regulate glycogen synthase phosphorylation and affinity for UDP-glucose in rat skeletal muscles. Am J Physiol Endocrinol Metab. 2007; 293(6):E1622–9. [PubMed: 17878227]

54. Ros S, et al. Control of liver glycogen synthase activity and intracellular distribution by phosphorylation. J Biol Chem. 2009; 284(10):6370–8. [PubMed: 19124463]

55. Nielsen JN, Wojtaszewski JF. Regulation of glycogen synthase activity and phosphorylation by exercise. Proc Nutr Soc. 2004; 63(2):233–7. [PubMed: 15294036]

56. Costa GL, et al. Site-directed mutagenesis using a rapid PCR-based method. Methods Mol Biol. 1996; 57:239–48. [PubMed: 8850010]

Highlights

- PSSM1-associated *GYS1* mutation causes constitutive enzyme activation.
- A conformational mechanism for this activation is proposed via in silico modeling.
- The mutant enzyme is highly active in the absence of its allosteric activator.
- The mutant enzyme does not respond appropriately to phosphorylation.

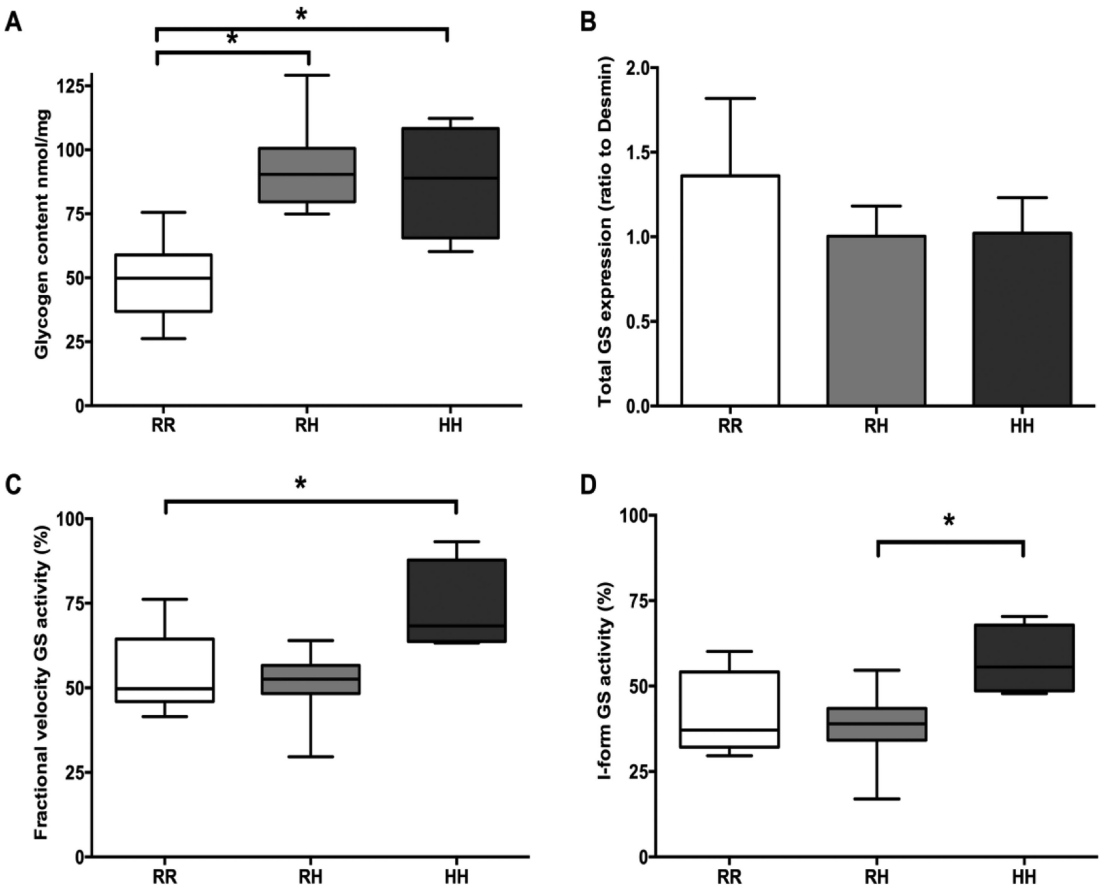

Figure 1.

A) Glycogen content of wet weight muscle samples from WT (RR)(n=7), PSSM1-heterozygotes (RH)(n=8) and PSSM1-homozygotes (HH)(n=4) horses (median +/− min/max values, box represents interquartile range; RR vs. RH p=0.005, RR vs. HH p= 0.041, *p<0.05). **B) Total glycogen synthase expression** in muscle homogenates from each of the genotypes was not significantly different (p=0.98). Glycogen synthase activity shown as C) fractional velocity (FV) and D) l-form activity. There was an increase in %FV between PSSM1-homozygotes (HH) and WT controls (RR) (p=0.03) and an increase in %I-form activity between heterozygotes (RH) and PSSM1-homozygotes (HH) samples (p=0.04) (median +/− min/max values, box represents interquartile range, RR (n= 12), RH (n=13), HH (n=4) *p<0.05**).**

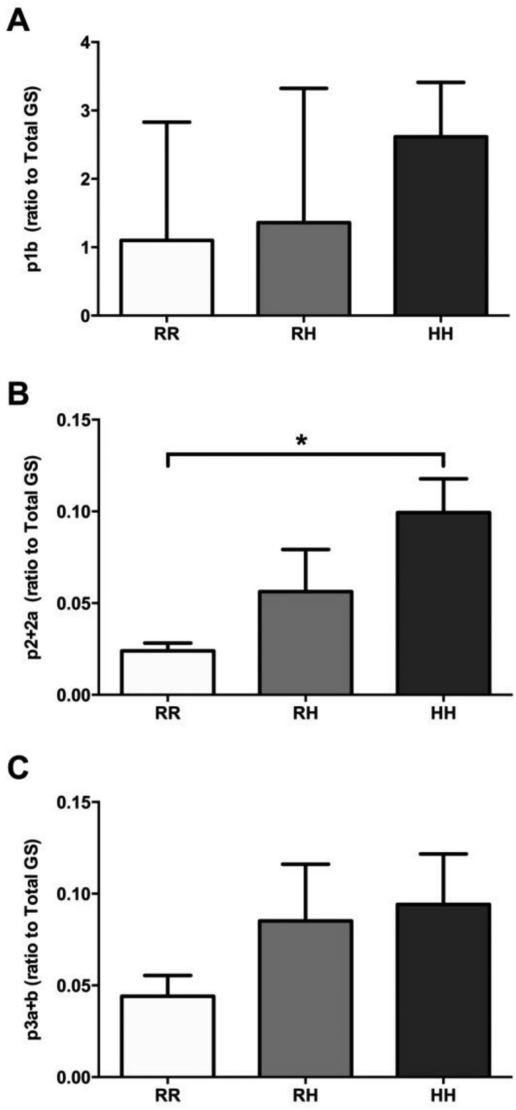

Figure 2. Western blot analysis of GS phosphorylation in skeletal muscle homogenates

There were no significant differences between the genotypes for phosphorylation of A) p1b isoform (p=0.48) and C) p3a+3b isoform (p=0.17). There was significantly increased phosphorylation at sites p2+2a (B) in PSSM1-homozygotes compared to control horses (RR) (p=0.009); (mean +/− SEM, RR (n=12) RH (n=13) HH (n=3) *p<0.05).

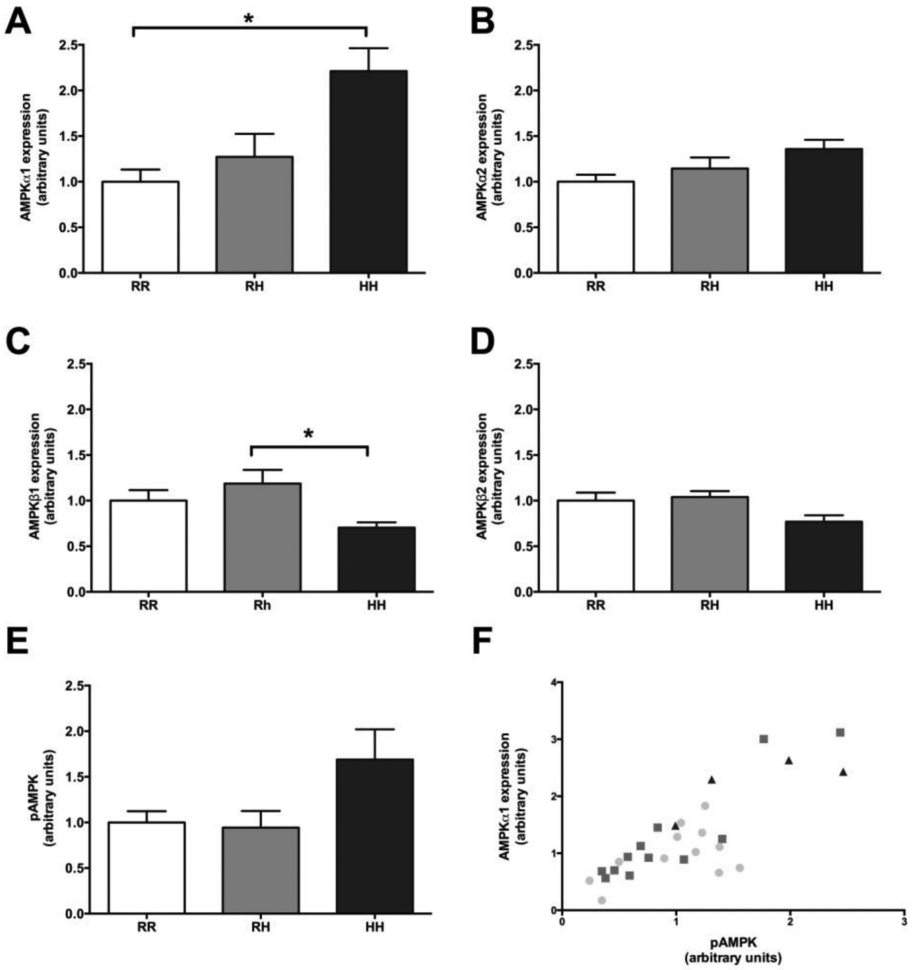

Figure 3. AMPK subunit expression and phosphorylation at Thr 172 from skeletal muscle extracts

There was a significant increase in AMPKα1 expression in PSSM1-homozygote samples (HH) compared to heterozygotes (RH) and WT controls (RR) (A; p=0.04) and a significant decrease in AMPKβ1 expression in the PSSM1-homozygote samples (HH) compared to the heterozygotes (C; p=0.03). There were no significant differences in AMPKα2 (p=0.15) or AMPKβ2 (p=0.28) expression between different genotypes (B and D). There was a significant and strong correlation between AMPKα1 and pAMPK expression (F; R^2=0.66, p<0.0001). (mean +/− SEM, RR (n=12) RH (n=13) HH (n=3) *p<0.05). Data for A to E is normalised to the mean of the WT control samples.

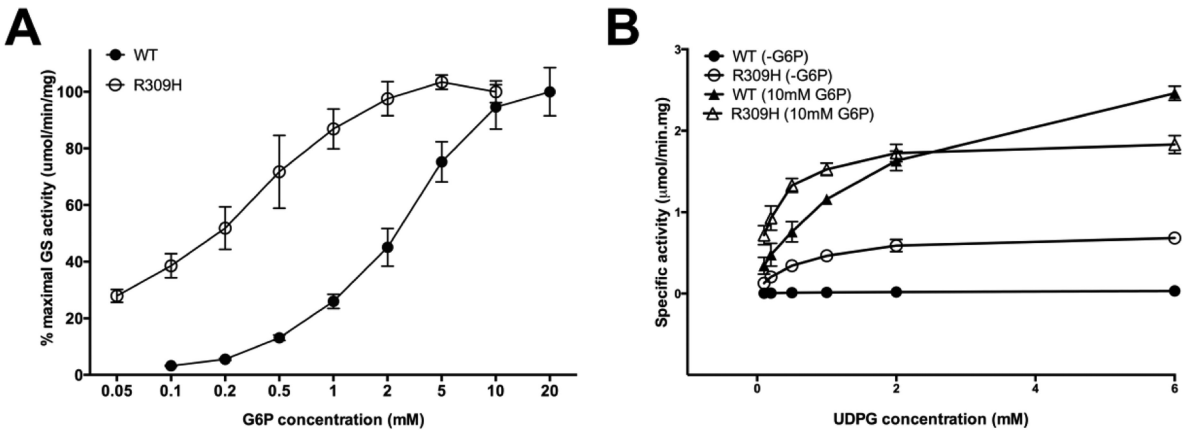

Figure 4. A) Glucose-6-phosphate and B) UDPG titration (with or without 10mM G6P) curves for WT and R309H mutant enzyme

These curves show that the mutant enzyme has much higher enzyme activity at much lower concentrations of G6P and reaches its maximal activity at much lower G6P concentrations (A). The mutant enzyme also has a higher affinity for UDPG (B). (Mean +/− SEM, n=3 repeats)

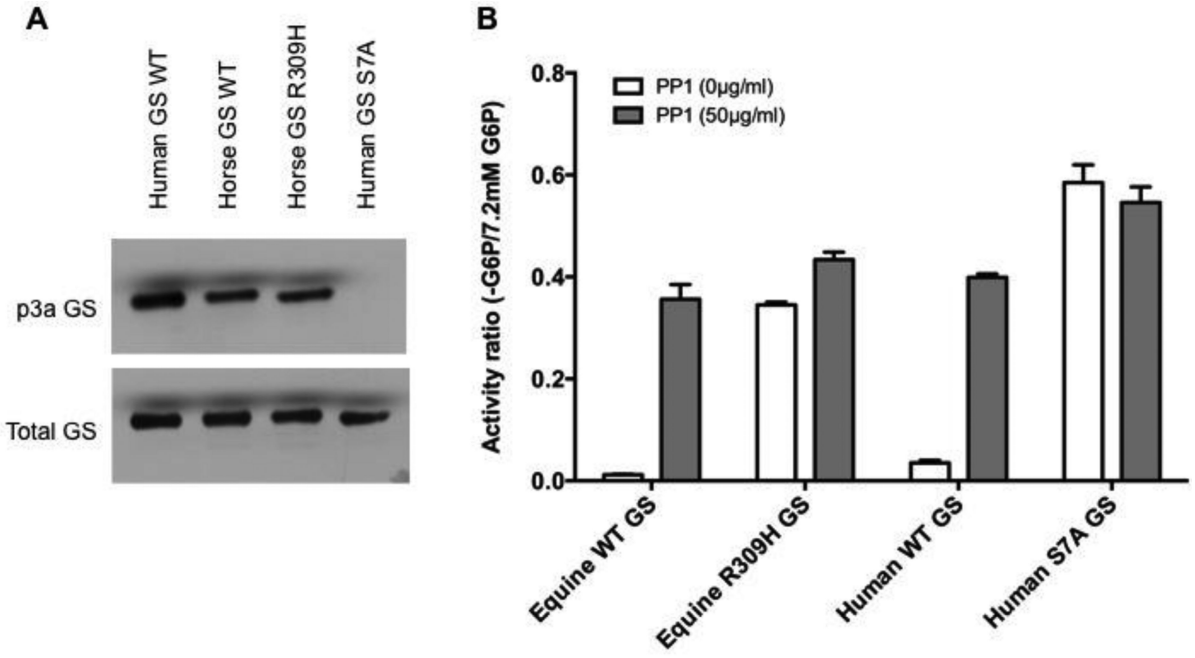

Figure 5. Phosphorylation (A) and Activity ratio (B) of insect derived WT and mutant (R309H) equine and human WT and S7A glycogen synthases

Activity ratio is minimal in both equine and human WT enzymes that are untreated with protein phosphatase 1 (PP1), but each WT enzymes' activity ratio increased when treated with the enzyme. In contrast, the equine mutant enzyme has a high ratio both with and without treatment with PP1 as also seen with the S7A human mutant GS, despite the equine mutant enzyme's phosphorylation. (n=3 replicates for each condition / enzyme; mean +/− SD).

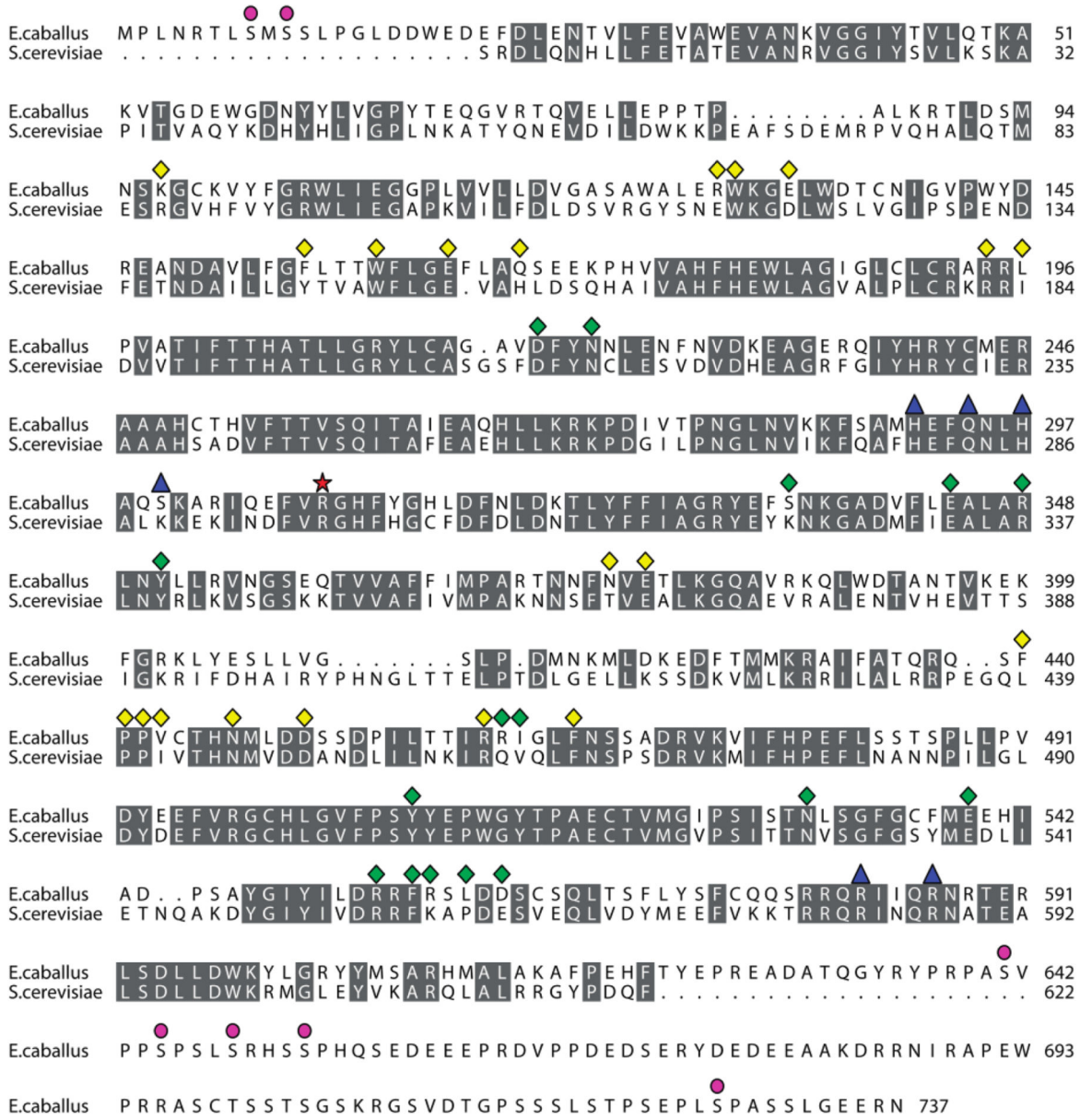

Figure 6. Sequence alignment of equine GS (Genbank accession ACB14276) and yeast Gsy2 (sequence in PDB ID 3NB0)

Red star: R309 in equine GS and the location of the PSSM1-associated R309H mutation. Magenta circles: predicted phosphorylation sites. Blue triangles: binding residues of glucose-6-phosphate. Diamonds: binding residues of maltodextrin (yellow: sites 1 and 2; green: sites 3 and 4).

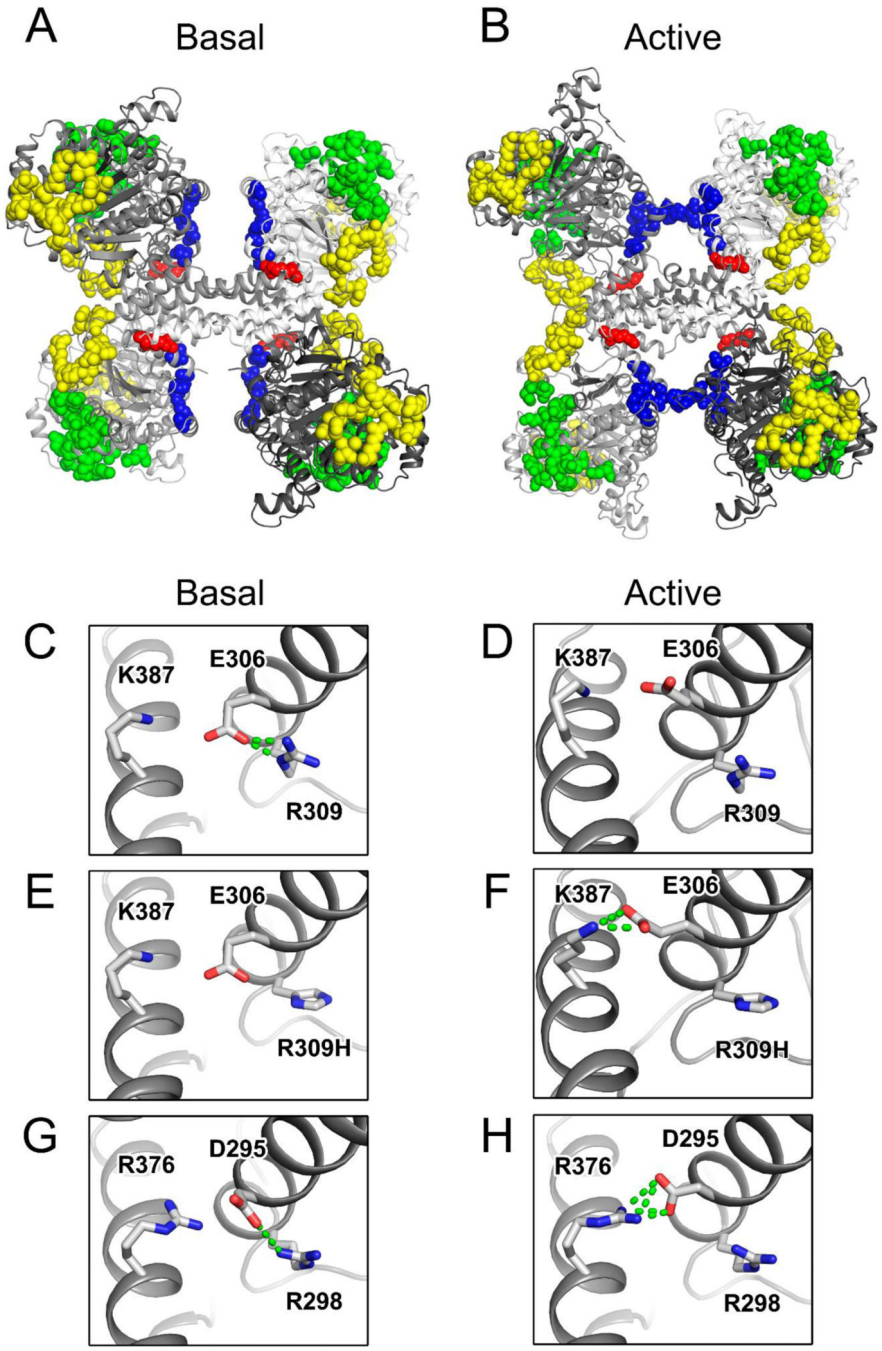

Figure 7. Homology models of equine GS

(A) Basal and (B) active-state equine WT GS model tetramers are shown as ribbons with monomers coloured different shades of grey. Residues in space-fill are R309 (red), G6P-binding contacts (blue) and maltodextrin-binding contacts (yellow: sites 1 and 2; green: sites 3 and 4). The 309 position and local charged residues are shown as sticks for WT GS [(C) basal; (D) active-state] and the PSSM1-associated R309H mutant [(E) basal; (F) active-

state]. Also shown as sticks are the corresponding residues in the crystal structures of yeast Gsy2p [(G) basal; (H) active-state]. Salt bridge interactions are shown as green dashes.

Table 1

Comparison of kinetics of WT and mutant (R309H) GS enzyme.

Protein	Km UDPG (mM) (-G6P)	Km UDPG (mM) (10mM G6P)	Vmax UDPG (μmol/min.mg) (-G6P)	Vmax UDPG (μmol/min.mg) (10mM G6P)	Vmax/Km (-G6P)	Vmax/Km (10mM G6P)	$S_{0.5}$ G6P (mM) (4.4mM UDPG)
WT GS	2.4 ±0.2	1.6 ±0.1	0.05 ±0.01	3.1 ±0.1	0.023 ±0.002	2.0 ±0.2	3.0 ±0.4
R309H GS	0.48 ±0.01	0.18 ±0.02	0.72 ±0.06	1.9 ±0.1	1.5 ±0.3	11 ±2	0.24 ±0.03

Values given are the mean ±SEM from 3 separate experiments.

Table 2

Specific activity of WT and R309H mutant GS in absence and presence of G6P (n=3).

	Specific activity –G6P (umol/min.mg)	Specific activity 10mM G6P (umol/min.mg)	Activity ratio
WT GS	0.04	2.33	0.02
R309H GS	0.36	1.06	0.34